ACS OMEGA

Open Access

http://pubs.acs.org/journal/acsodf

Article

Phthalocyanine Adsorbed on Monolayer CrI_3: Tailoring Their Magnetic Properties

Cihan Bacaksiz* and Maria Fyta

Cite This: *ACS Omega* 2024, 9, 34589−34596

Read Online

ACCESS | Metrics & More | Article Recommendations | Supporting Information

ABSTRACT: Metallo-phthalocyanines molecules, especially iron-phthalocyanines (Fe-Pc), are often examined due to their rich chemical, magnetic, and optoelectronic features. Due to these, Fe-Pc molecules are promising for applications in gas sensors, field-effect transistors, organic LEDs, and data storage. Motivated by this potential, this study investigates Fe-Pc molecules adsorbed on a magnetic monolayer, CrI_3. Using quantum-mechanical simulations, the aim of this work was to find pathways to selectively tune and engineer the magnetic and electronic properties of the molecules when they form hybrid complexes. The results quantitatively underline how adsorption alters the magnetic properties of the Fe-Pc molecules. Interestingly, the analysis points to changes in the molecular magnetic anisotropy when comparing the magnetic moment of the isolated molecule to that of the molecule/monolayer complex formed after adsorption. The presence of iodine vacancies was shown to enhance the magnetic interactions between the iron of the Fe-Pc molecule and the chromium of the monolayer. Our findings suggest ways to control oxygen capture−release properties through material choice and defect creation. Insights into the stability and charge density depletion on the molecule provide critical information for selective tuning of the magnetic properties and engineering of the functionalities of these molecule/material complexes.

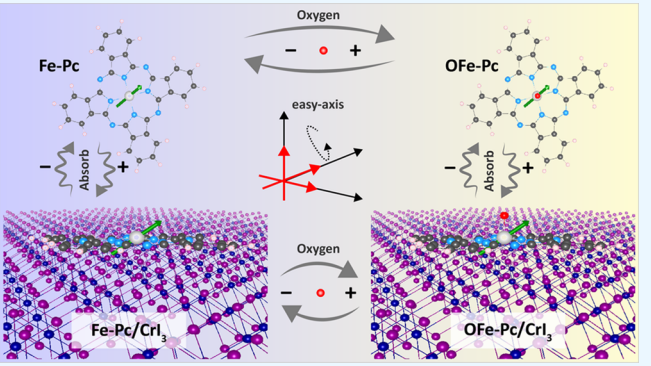

INTRODUCTION

Synthetic molecules such as phthalocyanines (Pc) have a structure similar to that of the natural porphyrins. These can also be found in the active site of many enzymes, such as hemoglobin. Enzymes are large molecules found in living organisms that act as catalysts in biological reactions. They are highly efficient due to their specificity for certain reactions, substrates, and regions within a molecule. They can repeat the same reaction multiple times without being altered. However, the surrounding environment, such as temperature and external electric or magnetic fields, can strongly influence their activity. Pc molecules exhibit structural and thermal stability.[1−4] It can also be combined with solid-state materials and can be adsorbed on these,[5−8] giving rise to applications in chemical sensors,[9] intrinsic semiconductors,[10] field-effect transistors,[11] organic light-emitting diodes,[12] and photovoltaic cells.[13]

In such setups, the type of the adsorbent surface is intuitively very important, since the interaction between molecules and such surfaces can be utilized for controlling the molecular properties and functions.[14,15] Atomically thin layers are particularly attractive due to their planarity aligned with the planarity in the Pc molecular structure as well as their controllable properties using external stimuli. Such materials have been studied extensively for their absorption properties.[16,17] It has also been shown that single molecules can modify their properties, such as band gap or magnetic anisotropy, in response to external factors such as temperature, light, or mechanical strain.[16−19] These properties are crucial for using molecules in devices, such as spin valves, or for magnetic storage. On top of this, Pc molecules are planar and can better adhere to different surfaces forming long-range structural patterns.[20−24] These characteristics allow for a control of the molecular properties for specific applications by modifying the properties of an underlying substrate, interface, or environment.[25−28] Various ways to control magnetic properties of these molecules are explored, such as selective modification of the spin-controlled ligand-field,[29,30] the molecule−surface magnetic exchange coupling,[31,32] or adding functional groups.[33] The strong spin−orbit coupling of certain types of atoms was also suggested as a means for controlling magnetization effects in complex materials.[34−36]

Received: March 20, 2024
Revised: June 28, 2024
Accepted: July 8, 2024
Published: July 29, 2024

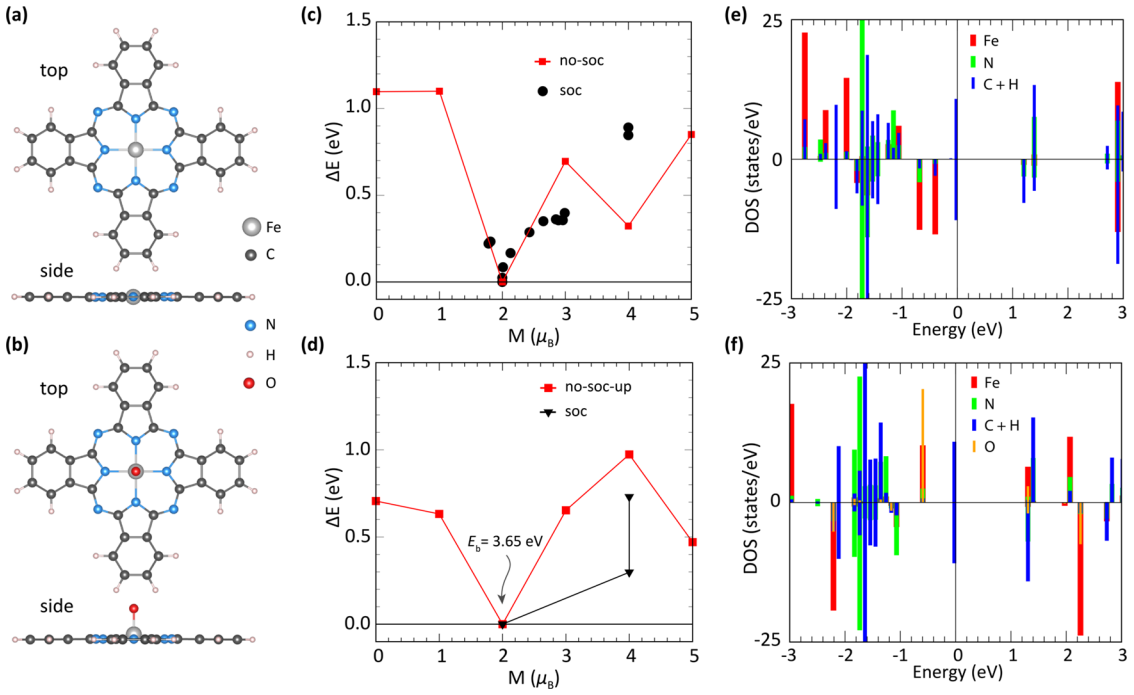

Figure 1. 'Top and side views of (a) Fe-Pc and (b) OFe-Pc, respectively. The color coding of the atoms is defined in the legends. The relative energy (ΔE) to the magnetic moment M (μ_B) for (c) Fe-Pc and (d) OFe-Pc. Panels (e) and (f) depict the atomic decomposition of the electronic density of states (DOS) of the minimum energy Fe-Pc and OFe-Pc structures, respectively. The data correspond to M = 2 μ_B.

Molecules, such as Pc, can be easily synthesized and are stable in an environment harsher than that within a living organism. Accordingly, they have the potential to be used to imitate the activity of biological molecules, such as enzymes, in solid-state setups for nanotechnological applications.[6,7] Especially, the structure of the Fe-Pc molecule is similar to the active site of hemoglobin which is responsible for holding oxygen and carbon dioxide in living organisms and hence capable of assisting release mechanisms. In order to explore and utilize the similarity of Fe-Pc to the active site of hemoglobin, we consider a controllable supporting layer that interacts with Fe-Pc. Typically, in such cases, single-layered (2D) materials are good candidates.[37−39] One of these, chromium iodide (CrI_3) is a single-layer magnet,[34] is structurally stable, and can provide a supporting layer for planar ligand surfaces. In addition, CrI_3 is ferromagnetic and can couple with the magnetization of the Fe-Pc molecule, while having tunable electronic and magnetic properties under the influence of external stimuli, such as strain and electric field.[36,40] A selective modification of magnetic anisotropy in Fe-Pc molecules has been previously demonstrated by Lisi et al., highlighting the role of structural symmetry disruption.[38] However, the potential effects of additional magnetic coupling between the Pc molecule and the underlying substrate, a scenario plausible with monolayer CrI_3, have not been explored in the existing literature. This can open up an additional way to control the properties of Pc molecules, broadening the options for its selective tuning. Motivated by all of these points, here, we investigate the possibility of utilizing the adsorption of Fe-Pc molecules on single-layer CrI_3 and targeted modification of the properties of the latter.

RESULTS AND DISCUSSION

Isolated Fe-Pc w/o Oxygen. We begin the analysis with isolated Pc molecules. The bare Fe-Pc molecule consists of Fe, C, N, and H atoms. The Fe atom is coordinated by four N atoms, forming a square planar structure, as shown in Figure 1a. C rings expand in those four directions and are also in a planar arrangement, and they are saturated with hydrogen atoms. The molecule is stable in different magnetic states of the Fe atom. Therefore, we have considered the different magnetic moments of the Fe atom in the structural optimizations with and without accounting for the spin−orbit coupling (SOC). In order to evaluate the influence of the SOC in the calculations, we present in Figure 1c, the energy difference with respect to the magnetic moment of the iron center. As the energy difference, we calculate the difference of the total energy of the system with respect to the lowest total energy of the same system with respect to the magnetic moment. In the following, we use this energy difference in order to quantify our results and refer to this as 'relative energy'. As observed in this figure, the minimum energy, which is ∼0.3 eV (without SOC) less than the second lowest one, is obtained for M = 2 μ_B in both cases. The magnetic anisotropy energy (MAE) is found to be 1.3 meV preferring the in-plane direction, as listed in Table 1. The magnetic anisotropy refers to the difference between the three different (x, y, and z) contributions to the direction of the magnetic moment. In Figure 1e, we show the atomic decomposition of the density of states as bars of different colors. The highest levels of the valence bands are occupied by the C + H states. The Fe states with little hybridization with the states from C, H, and N atoms correspond to the second and third highest levels.

In the case of the oxygen-bonded Fe-Pc (OFe-Pc), the single O atom corresponds to the fifth coordination of the Fe atom. There is a slight change in the position of the iron, which is shifted from the plane of the molecule toward the oxygen atom, as shown in Figure 1b (side view) and compared to the same view in Figure 1a. The N atoms and C ring remain planar. As in the bare Fe-Pc, the minimum energy structure is

https://doi.org/10.1021/acsomega.4c02708
ACS Omega 2024, 9, 34589−34596

Table 1. MAE of the Fe-Pc and OFe-Pc Molecules, as Denoted in the First Column[a]

	ΔE_x (meV)	ΔEy (meV)	ΔEz (meV)	M_{Fe} (μ_B)	E_b^O (eV)	E_g (eV)
Fe-Pc	0.0	0.0	1.3	2.0		1.22
OFe-Pc	0.7	0.0	2.4	2.0	3.65	1.33

[a] ΔE_x, ΔE_y, and ΔE_z are the relative energies with respect to the direction of the magnetic moment referring to the lowest energy, M_{Fe} is the magnetic moment of Fe atom, E_b^O is the oxygen binding energy, and E_g is the energy band gap of the molecule. The results in this and the following tables that refer to directional dependencies of the magnetic moment are the ones including SOC. The other properties that do not strongly depend on the magnetic moment direction as the ones without SOC.

obtained when the magnetic moment is 2 μ_B both in the calculations with and without SOC. As listed in Table 1, the MAE of OFe-Pc is slightly larger, 2.4 eV, yet also favors the in-plane direction. The binding energy of the O atom is found to be 3.65 eV, which is rather strong, especially compared to those of MAE. It should be noted that the binding energy is defined in eq 1, which refers the difference between the total energy of the molecule with oxygen to the molecule without oxygen and a single oxygen atom. Concluding this part referring to the isolated Fe-Pc molecules, the results strongly indicate that the magnetic moment of the Fe atom is not influenced—in magnitude—from its binding to oxygen and is directed in-plane, i.e., coplanar to the molecule plane. It should be noted that the ΔE_x = 0.7 is given in meV, thus can be considered as almost zero, taking into account the resolution of the DFT calculations and the error range expected. Both molecules show semiconducting properties, while the binding energy of O to Fe is relatively high, denoting a strong bond.

(O)Fe-Pc Adsorbed on Monolayer CrI_3. In order to selectively tune the oxygen binding utilizing the magnetic behavior of the Fe atom, we placed the molecule close to and on top of the surface of a magnetic CrI_3 monolayer. It was previously shown that the nonvanishing magnetization of CrI_3 at finite temperatures is due to strong spin−orbit coupling on I atoms rather than Cr atoms.[34−36] This suggests that any modification of magnetization affects the surface I atoms and any interacting components. The strong and robust magnetization, combined with the flat ligand surface, makes monolayer CrI_3 a perfect platform for the adsorption of Fe-Pc and the potential tuning of its magnetization and O binding properties. Although there are different possible arrangements of the Fe-Pc molecule on the supporting surface, such as the vertical one discussed in the case of graphene,[24] in this work, the plane of Fe-Pc is considered parallel to the plane of CrI_3. This parallel arrangement of the molecule to the surface maximizes the respective contact areas of the two parts, leading to stronger electronic and magnetic coupling.

As a first step, we have optimized the position and distance of the molecule and the monolayer (Fe-Pc/CrI_3), i.e., those positions corresponding to the minimum energy position. We considered a sufficiently large supercell of pristine monolayer CrI_3 and a grid-like lateral position of the atoms in CrI_3 as the initial positions of the Fe atom in Fe-Pc (refer to Figure 2a). Since the molecule and CrI_3 exhibit 4-fold and 3-fold symmetry, respectively, every 30° of rotation of the molecule generates equivalent arrangements of the two parts. Therefore, we considered rotations of 0° and 15° for the molecule relative

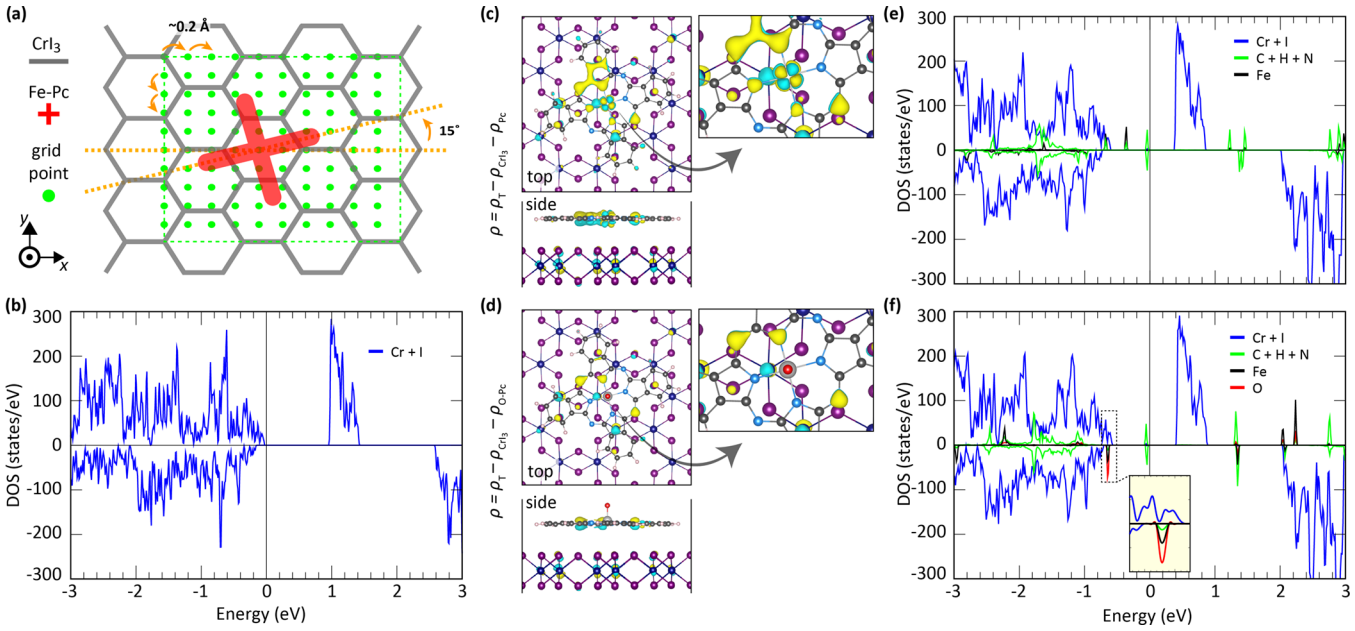

Figure 2. (a) Schematic representation (top view) of the considered position of Fe-Pc on the monolayer. The red crosses, gray lines, and green dots represent the Fe-Pc, CrI_3, and the considered positions of Fe-Pc on the CrI_3 lattice, respectively (see text for details). (b) Density of states of pristine CrI_3. Top and side views of the CDD of the molecule on the monolayer for (c) Fe-Pc and (d) OFe-Pc molecules. The density ρ on the y-axes corresponds to the CDD, with ρ_T, ρ_{CrI_3}, and $\rho_{Pc}(\rho_{O-Pc})$ as the charge density of the molecule/monolayer system, the isolated monolayer, and the isolated molecules. The insets on the right are zoomed-in regions of the CDDs. The color coding of the molecule is the same as that in Figure 1a, while the Cr and I atoms are colored purple and dark blue, respectively. For the CDD representation, the charge is being transferred from the cyan to the yellow regions. The density of state plots of (e) Fe-Pc and (f) OFe-Pc on CrI_3 are also depicted. The inset in (f) shows the zoomed-in region indicated by the dashed rectangle.

https://doi.org/10.1021/acsomega.4c02708
ACS Omega 2024, 9, 34589−34596

Table 2. Energetic Properties of the Fe-Pc and OFe-Pc Molecules on the Monolayer CrI_3, as Denoted in the First Column[a]

	ΔEx (meV)	ΔEy (meV)	ΔEz (meV)	M_{Fe} (μ_B)	E_{ads} (eV)	E_b^O (eV)	E_g^{cmplx} (eV)
Fe-Pc/CrI_3	18.1 (5.3)	13.2 (0.0)	0.0 (0.0)	2.0	1.94		1.27
OFe-Pc/CrI_3	11.7 (−1.0)	12.4 (−0.8)	0.0 (0.0)	2.0	1.90	3.60	1.36
Fe-Pc/d-CrI_3	15.9 (−0.8)	22.9 (3.7)	0.0 (0.0)	2.0	2.81		m
OFe-Pc/d-CrI_3	13.8 (−2.9)	16.9 (−2.3)	0.0 (0.0)	2.0	2.37	3.21	m

[a]The MAE, ΔE_x, ΔE_y, and ΔE_z, i.e., the relative energies with respect to the direction of the magnetic moment relative to the lowest energy, M_{Fe} the magnetic moment of Fe atom, E_{ads} the adsorption energy of the molecule on CrI_3, E_b^O the oxygen binding energy to Fe-Pc, and E_g^{cmplx}, and energy band gap of the molecule−monolayer complex are provided (see text for details). 'm' denotes a metallic behavior. In parentheses, the relative energies after subtracting the contribution related to the isolated CrI_3 (d-CrI_3) from that of the total system are provided.

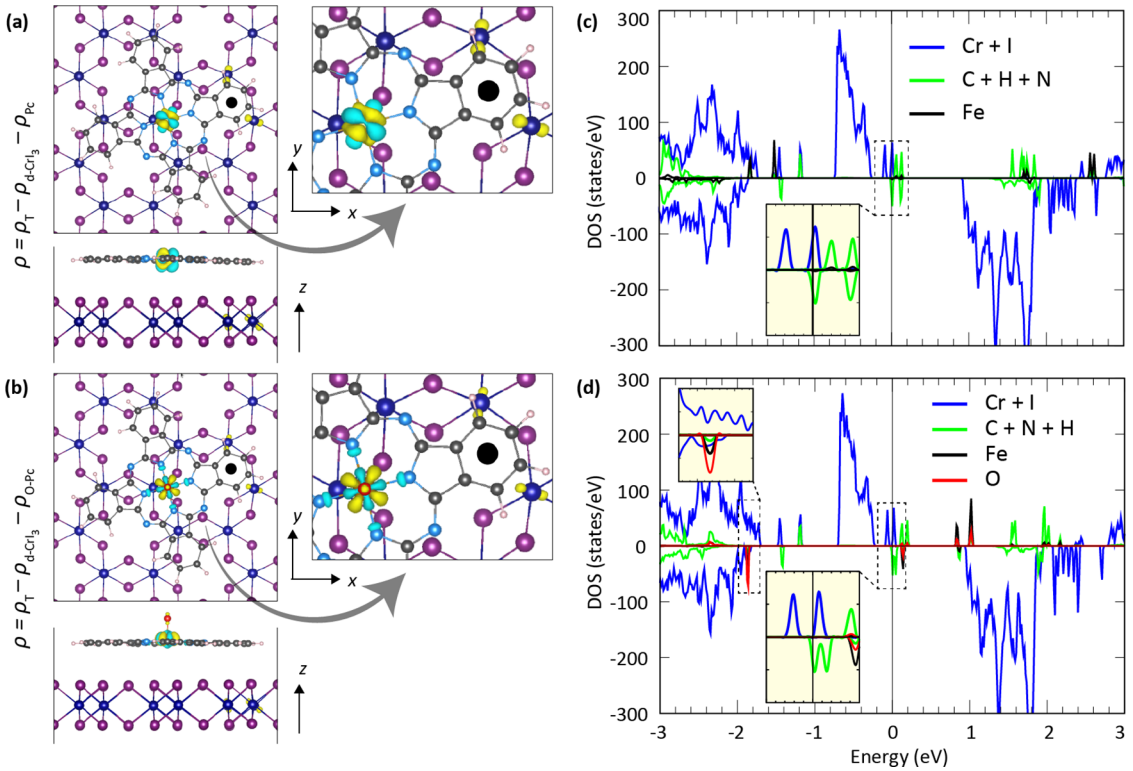

Figure 3. Charge density differences of (a) Fe-Pc and (b) OFe-Pc on d-CrI_3. The charge densities of pristine Fe-Pc (OFe-Pc) and d-CrI_3 are subtracted from the charge density of the combined molecule/monolayer case. The *y*-axes labeling corresponds to that of Figure 2. The black dot marks the position of the vacancy (the missing I atom). The electronic density of states (DOS) are provided for (c) Fe-Pc and (d) OFe-Pc on d-CrI_3. The insets in (c) and (d) show the zoomed-in regions in the dashed rectangles.

to the *x*-axis on the grid. Each generated structure was geometrically relaxed. In Figure 2c, the minimum energy position and corresponding charge density difference (CDD) are shown. The CDD is calculated as the addition of the charge densities of isolated CrI_3 and Fe-Pc subtracted from the charge density of the combined Fe-Pc/CrI_3. The electrons deplete from the cyan regions to the yellow regions, while Fe-Pc/CrI_3 is formed. The depletion is observed on the side of the molecule closer to the monolayer. A closer look to Fe reveals that the interaction between the molecule and monolayer changes the orbital occupancy of the Fe atoms. Regarding the CDD on CrI_3, there is a visible alternating (switching) charge depletion in the out-of-plane direction in the vicinity of the Fe-Pc molecule at both the I and Cr atoms. These changes are relatively local and less prominent compared to those observed on Fe-Pc. In Figure 2d, the CDD of OFe-Pc/CrI_3 is shown. In contrast to the Fe-Pc case, there is no difference obtained in the vicinity of the Fe atom of the isolated OFe-Pc molecule. However, the CDD in the oxygen case is more local than the Fe-Pc case, indicating that the presence of the binding of oxygen to the iron atom is strongly influencing its vicinity than the atoms further away. At the same time, the presence of the O−Fe bond hinders a stronger electron movement. On the CrI_3 side, the CDD becomes less prominent, implying that the interaction between Fe-Pc and CrI_3 is reduced in the case of O binding.

The far right panels of the same figure present the electronic density of states of the molecule/material complex. Compared to panel (b) of the pristine material, the overall signatures of the 2D material are kept intact. In the case of Fe-Pc adsorption, the iron atom mainly introduces a state below the Fermi level. When oxygen is bonded to the iron of the molecule, additional electronic states are provided, enhancing the anisotropy in the electronic structure. Specifically, the iron states of the Fe-Pc/CrI_3 complex are being hybridized with those of oxygen in the OFe-Pc/CrI_3 complex also providing additional states away from the Fermi level. Hence the Fe−O bond is enhancing the energy spectrum of the underlying material, providing a basis for tuning these properties. In order to support these findings, in Table 2, the magnetic anisotropy

https://doi.org/10.1021/acsomega.4c02708
ACS Omega 2024, 9, 34589−34596

of Fe-Pc/CrI_3 with and w/o oxygen is given. It is obvious that the magnetic moment of the total system prefers to point out-of-plane (in the *z*-direction). Based on Table 1 for the single molecule case, the in-plane direction is the favorite one. Accordingly, the magnetic anisotropy of CrI_3 should be subtracted from the total system. The respected relative anisotropy energies are given in the parentheses. Overall, the adsorption of the magnetic Fe-Pc molecule on the magnetic CrI_3 material changes the preferable direction of the magnetic moment of the Fe atom. The magnitude with 2 μ_B remains unmodified for the isolated molecules. However, its direction moves from the in-plane (*xy* plane) in the isolated case to the *yz* plane in the adsorbed case, i.e., the molecule/monolayer complex. In the OFe-Pc case, on the other hand, the preferable direction of the magnetic moment turns to in-plane (coplanar) as in the single OFe-Pc case; however, the MAE is slightly reduced. It should be noted that $\Delta E_{x(y)}$ is −1.0 (−0.8) meV after subtracting the CrI_3 contribution, which means that the MAE of OFe-Pc is more robust. Considering the fact that pristine CrI_3 and d-CrI_3 exhibit robust ferromagnetism and strong MAE in the out-of-plane direction,[36,41] we assume that the MAE of both individual pristine CrI_3 and d-CrI_3 remains as it is while forming the molecule/material complex. Interestingly, no significant change (only about 1%) was observed in the binding strength of oxygen to iron, denoting that the adsorption does not strongly influence this bond. The molecular/monolayer complex remains semiconducting with energy gaps close to those of the isolated molecules, as the respective differences are less than 4%. However, the fact that the O states are provided relatively close to the Fermi level denotes a possibility for further tuning of the electronic properties of the complex such as gating and applying external electric field that can affect the binding and MAE properties.

(O)Fe-Pc Adsorbed on Defective CrI_3. We further investigated the interactions of an Fe-Pc molecule on monolayer CrI_3 by including defects in the monolayer. As a representative defect, we remove one iodine(I) atom from the monolayer, forming a vacancy, and denote this defective monolayer as d-CrI_3. Throughout the synthesis, such defects are expected. On top of this, it is anticipated that dangling bonds due to the absence of an I atom in the vicinity of the Fe-Pc molecule can possibly lead to the formation of a covalent bond of the Fe-Pc and the defective monolayer, further modifying the properties of the whole and providing additional tuning pathways of the latter. It should be noted that the planar molecule and pristine 2D CrI_3 interact through van der Waals interactions. These limit to a certain extent the oxygen binding and the magnetic anisotropy strength. Regarding defective CrI_3 individually, it has been previously shown that an I vacancy enhances magnetic anisotropy, strengthens ferromagnetic interactions between Cr atoms, and increases the magnetic moment of Cr atoms near the vacancy.[42,43] Our results confirm these findings (see the Supporting Information). In order to better assess the defective monolayer case and its interaction with the molecule, we have constructed a different d-CrI_3 monolayer by removing each time one I atom at a different position in the monolayer. The position of the molecule is optimized similarly to the pristine (no-defect) case in the previous section. In Figure 3, the energetically favorable defective structures are shown with the CDD and the missing I atom represented by a black dot. The CDDs for both molecules adsorbed on the monolayer are very similar, with that of OFe-Pc/d-CrI_3 being slightly more concentrated toward the O atom. On the CrI_3 side, the CDD is localized on two Cr atoms in the vicinity of the I vacancy and shows slight changes moving from Fe-Pc/d-CrI_3 to O-bonded OFe-Pc/d-CrI_3. This points directly to the fact that changes in the electronic and magnetic anisotropy properties are found on the Fe-Pc(OFe-Pc) part.

A closer check of the molecular planarity reveals that the molecule leans toward the 2D material at the vacancy position, locally destroying its planarity. This effect is less strong in the presence of the oxygen atom (OFe-Pc/d-CrI_3), denoting that the O−Fe binding counterbalances the reduced dispersion interactions of the molecule and the monolayer in the vicinity of the defect. Overall, the CDD underlines tunable changes in the Fe-related energy levels when this is bonded to the oxygen atom (compare black lines in panels (c) and (d) of the figure). In (d), the O−Fe binding provides hybridized electronic states, removing the original Fe states in (c). The former are now deeper below the Fermi level, while new Fe + O states are provided above the Fermi level. These could potentially be further tuned and shifted by accounting for additional or other defects.

Defect-Dependent Modifications in the Magnetic Properties of the Complex. In order to unravel the influence of the defect in the properties of the molecule/material complex, we carefully examine the differences in both the CDD and electronic density of states of these systems with and without the CrI_3 defect. For this comparison, we refer to Figures 2 and 3. Inspection of the CDD in these figures reveals that in both cases, the CDD mainly concentrates on the molecules. In the pristine material, CDD signatures are also seen on the Cr atoms in the material. At the same time, the CDD is more spread-out than in the defective case, in which the CDD is more localized, denoting an accumulation closer to Fe and O−Fe. Due to the presence of the defect, the depletion on the lower part of the molecule, which interacts stronger with the monolayer, is lower than in the pristine (non-defective) case. Comparing the structural properties reveals that the molecule remains planar in the pristine CrI_3, while it shows an off-planar structure in the d-CrI_3, especially in the Fe-Pc molecules (see Discussion above). The adsorption of the molecule is significantly stronger in the defective case, as evidenced from the considerable increase of 25−45% in the adsorption energy of the molecule to the monolayer. It should be noted that the adsorption energy was calculated as $E_{ads} = E_{2D} + E_{mol} - E_{cmplx}$, where E_{2D} and E_{mol} are the total energies of the isolated monolayer and molecule, respectively, while E_{cmplx} is the total energy of the complex, including the molecule adsorbed on the monolayer. At the same time, the oxygen binding to Fe-Pc becomes slightly weaker, as its binding energy decreases about 10%.

Turning to the electronic density of states reveals some more pronounced differences between the pristine and defective materials for both types of Pc molecules considered. The presence of the defect introduces electronic states around the Fermi level, which would be very practical in applications, as these states would be easier to tune and selectively modified. In Fe-Pc/d-CrI_3, the iron states move deeper below the Fermi level, while in the pristine material, these are closed to the Fermi energy. Looking into the effect of the oxygen atom in both the OFe-Pc/CrI_3 and OFe-Pc/d-CrI_3 complexes, the Fe and O states do hybridize in both and provide additional states in a way that enhances the anisotropy of the system. However, these states are much closer to the Fermi level in the defective

https://doi.org/10.1021/acsomega.4c02708
ACS Omega 2024, 9, 34589−34596

cases than in the pristine case. Accordingly, the presence of the defect again provides a better template for further tuning. Overall, the presence of the defect shifts the conducting properties of the complex from semiconducting to metallic. Interestingly, the magnetic properties of the complex compared to the isolated parts were modified in a way that the preferable direction of the magnetic moment was changed from in- to out-of-plane. For both the pristine and the defective CrI_3, the magnetic moment turned to noncoplanar to the planes of both the molecule and the material. Experimental validation of these findings would be feasible and highly valuable. Verifying the shift in electronic properties and especially the change in the magnetic anisotropy through experimental techniques will provide additional insights. Supported by the theoretical trends, these would allow further exploration of how external stimuli can be used to realize applications in electronics. Such a combined experimental and theoretical validation has the potential to uncover new phenomena associated with defect-induced modifications and an understanding of such hybrid complexes. However, an interesting observation toward further selective tuning was observed when subtracting the contribution of the isolated monolayer (see Table 2. In the pristine CrI_3 and the Fe-Pc molecules, the magnetic direction prefers the *y*- and *z*-directions and not the *x*-direction (see figures for the axes notation). When oxygen is added to Fe-Pc, this is reversed, as the relative energies of the *x*- and *y*- directions are preferable compared to the *z*-component, and the magnetic moment is actually in-plane. Similar are the observations for the defective case, as again removing the monolayer contribution denotes that the *x*-component is preferable over the other two. In the end, the incorporation of the O atom enhances the planarity of the magnetic moment.

CONCLUSIONS

Using quantum-mechanical simulations, we have modeled the adsorption of an Fe-Pc molecule on a two-dimensional CrI_3 material. Both isolated Fe-Pc and OFe-Pc exhibit strong magnetic moments parallel to the plane of the molecule, though the magnetic anisotropy for the oxygen-bonded case (OFe-Pc) slightly increases. When these molecules are adsorbed on 2D CrI_3, the preferable direction of the total magnetic moment turns perpendicular to both the plane of the molecule and the material. Considering the (O)Fe-Pc individually, by removing the energetic contribution of the 2D layer, reveals that each complex of interest exhibits a unique preferable direction for its magnetic moment. The complex Fe-Pc/CrI_3 prefers the *yz* plane, Fe-Pc/d-CrI_3 the *x*-direction, while OFe-Pc/CrI_3 and 0Fe-Pc/d-CrI_3 resemble the cases of the isolated molecules. The presence of the Fe-Pc molecules enhances the energy spectrum of the pristine material, while the additional O in OFe-Pc further allows the selective tuning of the Fe states, enhancing the magnetic anisotropy with respect to the Fe-Pc adsorbed on CrI_3. Introducing a defect in the 2D material further enhances the available electronic states around the Fermi level. Again, the binding of oxygen to the iron atom in the adsorption of OFe-Pc provides hybridized states that are shifted with respect to the Fe states in defective Fe-Pc/d-CrI_3.

Using these molecules and materials to form hybrid complexes, we have provided pathways for modifying their electronic structure and magnetic anisotropy. It was observed that a stronger adsorption (in the defective monolayer case) reduces the binding strength of oxygen to the molecule, indicating that the oxygen release could be tuned through a selective engineering of the molecules, materials, and defects. At the same time, the directionality of the magnetic moment of the iron atom could also be tailored due to the adsorption process modifying the in-plane direction to an out-of-plane one. The presence of oxygen could reduce these differences. On the same ground, the analysis of the influence of the monolayer on this anisotropy leads to an assessment of its influence opening ways for further tuning. Our results have emphasized the interplay of all the components in the hybrid complexes, allowing the design of such hybrids. Toward this, we emphasize the large phase space (molecule, material, and defect type) for further tuning and tailoring their functionalities. This deeper understanding of the inherent interactions of single atoms as well as the influence and distinct roles of the molecular and material part provides valuable insights for tailoring properties and functions in view of targeted applications.

COMPUTATIONAL DETAILS

In order to investigate the structural, electronic, and magnetic properties, we perform calculations based on the density functional theory (DFT). For this, the Vienna ab initio simulation package (VASP)[44−46] was used. This solves the Kohn−Sham equations iteratively using a plane-wave basis set. It has been shown that for hybrid systems, such as those consisting of a molecule and surface or 2D materials, as well as individual 2D materials, the Perdew−Burke−Ernzerhof (PBE) form of the generalized gradient approximation (GGA)[47] generates reliable results.[21,24,35,36,48] Considering the balance between computational cost and accuracy as well as the frequent use of GGA-based functionals for similar systems in the literature, we have adopted the PBE form of the GGA to describe the electron exchange and correlation properties. The van der Waals (vdW) forces were taken into account using the DFT-D2 method of Grimme.[49] The kinetic energy cutoff of the plane-wave basis set and the energy convergence criterion in the ground-state calculations were set at 500 eV and 10^{-5} eV, respectively. A Gaussian smearing of 0.01 eV was used, and the pressures on the unit cell were decreased to a value lower than 1.0 kbar in all three directions. The on-site Coulomb repulsion[50] parameters, *U*, were taken as 4.00 and 2.65 eV for the magnetic Fe and Cr atoms, respectively.[51−53] In order to avoid interactions between periodically repeated images of the computational box (molecule and monolayer), calculations were performed with a sufficiently large vacuum space of ∼15 Å in the direction perpendicular to the monolayer.

The DFT simulations discussed above were applied on the single-isolated Fe-Pc molecules, with and without an oxygen (referring to Fe-Pc and OFe-Pc, respectively), as well as on these molecules as adsorbed on the monolayer CrI_3. The binding energy of oxygen is calculated using the following equation:

$$E_b^O = E_T^{no\text{-}O} + E_O - E_T^{w\text{-}O} \quad (1)$$

where $E_T^{no\text{-}O}$, E_O, and $E_T^{w\text{-}O}$ stand for the total energy system without O, the energy of the single O atom, and the total energy of the system with O, respectively. The adsorption energy of Fe-Pc (OFe-Pc) on the 2D layer is calculated using the following equation:

$$E_{ads} = E_{2D} + E_{mol} - E_{cmplx} \quad (2)$$

https://doi.org/10.1021/acsomega.4c02708
ACS Omega 2024, 9, 34589−34596

where E_{mol}, E_{2D}, and E_{cmplx} represent the energy of the molecule, (2D) monolayer CrI_3 (defective CrI_3), and molecule/monolayer complex, respectively. These systems were modeled twice, once including SOC and once without SOC. We will refer to these in the following as 'SOC' and 'noSOC' simulations, respectively. The simulations provide an insight into the electronic and magnetic properties of both the single molecules, as well as their combination, i.e., adsorption, on the 2D CrI_3 materials. Based on the aforementioned considerations, we calculate and refer to the magnetic anisotropy energy (MAE) as the main indicator of how the system responds energetically to the direction of the spin alignment.

■ ASSOCIATED CONTENT

Supporting Information

The Supporting Information is available free of charge at https://pubs.acs.org/doi/10.1021/acsomega.4c02708.

Details of the structural and magnetic optimizations for single Fe-Pc and OFe-Pc, pristine CrI_3, and I atom vacant CrI_3; and additional insights into the robustness of the density of states of Fe-Pc/CrI_3 for different positions of Fe-Pc (PDF)

■ AUTHOR INFORMATION

Corresponding Author

Cihan Bacaksiz − *Department of Physics & NANOlab Center of Excellence, University of Antwerp, B-2020 Antwerp, Belgium; Computational Biotechnology, RWTH Aachen University, 70574 Aachen, Germany;* orcid.org/0000-0003-1818-5835; Email: cihan.bacaksiz@uantwerpen.be

Author

Maria Fyta − *Computational Biotechnology, RWTH Aachen University, 70574 Aachen, Germany*

Complete contact information is available at: https://pubs.acs.org/10.1021/acsomega.4c02708

Notes

The authors declare no competing financial interest.

■ ACKNOWLEDGMENTS

The authors gratefully acknowledge the computing time provided to them at the NHR Center NHR4CES at RWTH Aachen University (project number p0020207). This is funded by the Federal Ministry of Education and Research and the state governments participating on the basis of the resolutions of the GWK for national high-performance computing at universities. The computational resources and services used in this work were also provided by the VSC (Flemish Supercomputer Center), funded by Research Foundation-Flanders (FWO).

■ REFERENCES

(1) Lucia, E. A.; Verderame, F. D. Spectra of polycrystalline phthalocyanines in the visible region. *J. Chem. Phys.* **1968**, *48*, 2674−2681.

(2) Edwards, L.; Gouterman, M. Porphyrins: XV. Vapor absorption spectra and stability: Phthalocyanines. *J. Mol. Spectrosc.* **1970**, *33*, 292−310.

(3) Endo, A.; Matsumoto, S.; Mizuguchi, J. Interpretation of the near-infrared absorption of magnesium phthalocyanine complexes in terms of exciton coupling effects. *J. Phys. Chem. A* **1999**, *103*, 8193−8199.

(4) Salomon, E.; Papageorgiou, N.; Ferro, Y.; Layet, J. Electronic transitions and resonance electron scattering measured by electron energy loss spectroscopy of lead phthalocyanine thin film. *Thin Solid Films* **2004**, *466*, 259−264.

(5) Lu, X.; Hipps, K.; Wang, X.; Mazur, U. Scanning tunneling microscopy of metal phthalocyanines: d7 and d9 cases. *J. Am. Chem. Soc.* **1996**, *118*, 7197−7202.

(6) Nazin, G.; Qiu, X.; Ho, W. Visualization and spectroscopy of a metal-molecule-metal bridge. *Science* **2003**, *302*, 77−81.

(7) Gottfried, J. M. Surface chemistry of porphyrins and phthalocyanines. *Surf. Sci. Rep.* **2015**, *70*, 259−379.

(8) Zhao, A.; Hu, Z.; Wang, B.; Xiao, X.; Yang, J.; Hou, J. Kondo effect in single cobalt phthalocyanine molecules adsorbed on Au(111) monoatomic steps. *J. Chem. Phys.* **2008**, *128*, 234705.

(9) Angione, M. D.; Pilolli, R.; Cotrone, S.; Magliulo, M.; Mallardi, A.; Palazzo, G.; Sabbatini, L.; Fine, D.; Dodabalapur, A.; Cioffi, N.; Torsi, L. Carbon based materials for electronic bio-sensing. *Mater. Today* **2011**, *14*, 424−433.

(10) Papageorgiou, N.; Salomon, E.; Angot, T.; Layet, J.-M.; Giovanelli, L.; Le Lay, G. Physics of ultra-thin phthalocyanine films on semiconductors. *Prog. Surf. Sci.* **2004**, *77*, 139−170.

(11) Bao, Z.; Lovinger, A. J.; Dodabalapur, A. Organic field-effect transistors with high mobility based on copper phthalocyanine. *Appl. Phys. Lett.* **1996**, *69*, 3066−3068.

(12) Nguyen, T.-P. Polymer-based nanocomposites for organic optoelectronic devices A review. *Surf. Coat. Technol.* **2011**, *206*, 742−752.

(13) Peumans, P.; Forrest, S. Very-high-efficiency double-heterostructure copper phthalocyanine/C 60 photovoltaic cells. *Appl. Phys. Lett.* **2001**, *79*, 126−128.

(14) Liu, W.; Tkatchenko, A.; Scheffler, M. Modeling adsorption and reactions of organic molecules at metal surfaces. *Accounts of chemical research* **2014**, *47*, 3369−3377.

(15) Hermann, J.; DiStasio, R. A., Jr; Tkatchenko, A. First-principles models for van der Waals interactions in molecules and materials: Concepts, theory, and applications. *Chem. Rev.* **2017**, *117*, 4714−4758.

(16) Chaves, A.; Azadani, J. G.; Alsalman, H.; Da Costa, D.; Frisenda, R.; Chaves, A.; Song, S. H.; Kim, Y. D.; He, D.; Zhou, J.; Castellanos-Gomez, A.; Peeters, F. M.; Liu, Z.; Hinkle, C. L.; Oh, S.-H.; Ye, P. D.; Koester, S. J.; Lee, Y. H.; Avouris, P.; Wang, X.; Low, T. Bandgap engineering of two-dimensional semiconductor materials. *npj 2D Mater. Appl.* **2020**, *4*, 29.

(17) Brill, A. R.; Koren, E.; de Ruiter, G. Molecular functionalization of 2D materials: from atomically planar 2D architectures to off-plane 3D functional materials. *Journal of Materials Chemistry C* **2021**, *9*, 11569−11587.

(18) Dai, Z.; Liu, L.; Zhang, Z. Strain engineering of 2D materials: issues and opportunities at the interface. *Adv. Mater.* **2019**, *31*, No. 1805417.

(19) Stróżecka, A.; Soriano, M.; Pascual, J.; Palacios, J. Reversible change of the spin state in a manganese phthalocyanine by coordination of CO molecule. *Phys. Rev. Lett.* **2012**, *109*, No. 147202.

(20) Betti, M. G.; Gargiani, P.; Frisenda, R.; Biagi, R.; Cossaro, A.; Verdini, A.; Floreano, L.; Mariani, C. Localized and dispersive electronic states at ordered FePc and CoPc chains on Au (110). *J. Phys. Chem. C* **2010**, *114*, 21638−21644.

(21) Cheng, Z.; Gao, L.; Deng, Z.; Jiang, N.; Liu, Q.; Shi, D.; Du, S.; Guo, H.; Gao, H.-J. Adsorption behavior of iron phthalocyanine on Au (111) surface at submonolayer coverage. *J. Phys. Chem. C* **2007**, *111*, 9240−9244.

(22) Gopakumar, T.; Brumme, T.; Kroger, J.; Toher, C.; Cuniberti, G.; Berndt, R. Coverage-driven electronic decoupling of Fe-phthalocyanine from a Ag (111) substrate. *J. Phys. Chem. C* **2011**, *115*, 12173−12179.

(23) Mao, J.; Zhang, H.; Jiang, Y.; Pan, Y.; Gao, M.; Xiao, W.; Gao, H.-J. Tunability of supramolecular kagome lattices of magnetic

phthalocyanines using graphene-based moiré patterns as templates. *J. Am. Chem. Soc.* **2009**, *131*, 14136−14137.
(24) Zemła, M. R.; Czelej, K.; Majewski, J. A. Graphene−iron (II) phthalocyanine hybrid systems for scalable molecular spintronics. *J. Phys. Chem. C* **2020**, *124*, 27645−27655.
(25) Gottfried, M.; Marbach, H. Surface-confined coordination chemistry with porphyrins and phthalocyanines: aspects of formation, electronic structure, and reactivity. *Zeitschrift für Physikalische Chemie* **2009**, *223*, 53−74.
(26) Hieringer, W.; Flechtner, K.; Kretschmann, A.; Seufert, K.; Auwarter, W.; Barth, J. V.; Gorling, A.; Steinruck, H.-P.; Gottfried, J. M. The surface trans effect: influence of axial ligands on the surface chemical bonds of adsorbed metalloporphyrins. *J. Am. Chem. Soc.* **2011**, *133*, 6206−6222.
(27) Ballav, N.; Wackerlin, C.; Siewert, D.; Oppeneer, P. M.; Jung, T. A. Emergence of on-surface magnetochemistry. *J. Phys. Chem. Lett.* **2013**, *4*, 2303−2311.
(28) Peisert, H.; Uihlein, J.; Petraki, F.; Chassé, T. Charge transfer between transition metal phthalocyanines and metal substrates: The role of the transition metal. *J. Electron Spectrosc. Relat. Phenom.* **2015**, *204*, 49−60.
(29) Bhandary, S.; Ghosh, S.; Herper, H.; Wende, H.; Eriksson, O.; Sanyal, B. Graphene as a reversible spin manipulator of molecular magnets. *Physical review letters* **2011**, *107*, No. 257202.
(30) Bhandary, S.; Brena, B.; Panchmatia, P. M.; Brumboiu, I.; Bernien, M.; Weis, C.; Krumme, B.; Etz, C.; Kuch, W.; Wende, H.; Eriksson, O.; Sanyal, B. Manipulation of spin state of iron porphyrin by chemisorption on magnetic substrates. *Phys. Rev. B* **2013**, *88*, No. 024401.
(31) Bhandary, S.; Eriksson, O.; Sanyal, B. Defect controlled magnetism in FeP/graphene/Ni(111). *Sci. Rep.* **2013**, *3*, 3405.
(32) Herper, H. C.; Bernien, M.; Bhandary, S.; Hermanns, C. F.; Krüger, A.; Miguel, J.; Weis, C.; Schmitz-Antoniak, C.; Krumme, B.; Bovenschen, D.; Tieg, C.; Sanyal, B.; Weschke, E.; Czekelius, C.; Kuch, W.; Wende, H.; Eriksson, O. Iron porphyrin molecules on Cu(001): Influence of adlayers and ligands on the magnetic properties. *Phys. Rev. B* **2013**, *87*, No. 174425.
(33) Wäckerlin, C.; Chylarecka, D.; Kleibert, A.; Müller, K.; Iacovita, C.; Nolting, F.; Jung, T. A.; Ballav, N. Controlling spins in adsorbed molecules by a chemical switch. *Nat. Commun.* **2010**, *1*, 61.
(34) Huang, B.; Clark, G.; Navarro-Moratalla, E.; Klein, D. R.; Cheng, R.; Seyler, K. L.; Zhong, D.; Schmidgall, E.; McGuire, M. A.; Cobden, D. H.; Yao, W.; Xiao, D.; Jarillo-Herrero, P.; Xu, X. Layer-dependent ferromagnetism in a van der Waals crystal down to the monolayer limit. *Nature* **2017**, *546*, 270−273.
(35) Lado, J. L.; Fernández-Rossier, J. On the origin of magnetic anisotropy in two dimensional CrI3. *2D Materials* **2017**, *4*, No. 035002.
(36) Bacaksiz, C.; Šabani, D.; Menezes, R.; Milošević, M. Distinctive magnetic properties of Cr I 3 and Cr Br 3 monolayers caused by spin-orbit coupling. *Phys. Rev. B* **2021**, *103*, No. 125418.
(37) Haldar, S.; Bhandary, S.; Vovusha, H.; Sanyal, B. Comparative study of electronic and magnetic properties of iron and cobalt phthalocyanine molecules physisorbed on two-dimensional MoS 2 and graphene. *Phys. Rev. B* **2018**, *98*, No. 085440.
(38) Lisi, S.; Gargiani, P.; Scardamaglia, M.; Brookes, N. B.; Sessi, V.; Mariani, C.; Betti, M. G. Graphene-induced magnetic anisotropy of a two-dimensional iron phthalocyanine network. *J. Phys. Chem. Lett.* **2015**, *6*, 1690−1695.
(39) Yin, H.; Lin, H.; Zhang, Y.; Huang, S. Iron (II) Phthalocyanine Adsorbed on Defective Graphenes: A Density Functional Study. *ACS omega* **2022**, *7*, 43915−43922.
(40) Vishkayi, S. I.; Torbatian, Z.; Qaiumzadeh, A.; Asgari, R. Strain and electric-field control of spin-spin interactions in monolayer CrI 3. *Physical Review Materials* **2020**, *4*, No. 094004.
(41) Menezes, R. M.; Šabani, D.; Bacaksiz, C.; de Souza Silva, C. C.; Milošević, M. V. Tailoring high-frequency magnonics in monolayer chromium trihalides. *2D Materials* **2022**, *9*, No. 025021.
(42) Zhao, Y.; Lin, L.; Zhou, Q.; Li, Y.; Yuan, S.; Chen, Q.; Dong, S.; Wang, J. Surface vacancy-induced switchable electric polarization and enhanced ferromagnetism in monolayer metal trihalides. *Nano Lett.* **2018**, *18*, 2943−2949.
(43) Wang, R.; Su, Y.; Yang, G.; Zhang, J.; Zhang, S. Bipolar doping by intrinsic defects and magnetic phase instability in monolayer CrI3. *Chem. Mater.* **2020**, *32*, 1545−1552.
(44) Kresse, G.; Hafner, J. Ab initio molecular dynamics for liquid metals. *Phys. Rev. B* **1993**, *47*, 558.
(45) Kresse, G.; Furthmüller, J. Efficiency of ab-initio total energy calculations for metals and semiconductors using a plane-wave basis set. *Computational materials science* **1996**, *6*, 15−50.
(46) Kresse, G.; Furthmüller, J. Efficient iterative schemes for ab initio total-energy calculations using a plane-wave basis set. *Phys. Rev. B* **1996**, *54*, 11169.
(47) Perdew, J. P.; Burke, K.; Ernzerhof, M. Generalized gradient approximation made simple. *Physical review letters* **1996**, *77*, 3865.
(48) Kartsev, A.; Augustin, M.; Evans, R. F.; Novoselov, K. S.; Santos, E. J. Biquadratic exchange interactions in two-dimensional magnets. *npj Comput. Mater.* **2020**, *6*, 150.
(49) Grimme, S. Semiempirical GGA-type density functional constructed with a long-range dispersion correction. *Journal of computational chemistry* **2006**, *27*, 1787−1799.
(50) Dudarev, S. L.; Botton, G. A.; Savrasov, S. Y.; Humphreys, C.; Sutton, A. P. Electron-energy-loss spectra and the structural stability of nickel oxide: An LSDA+ U study. *Phys. Rev. B* **1998**, *57*, 1505.
(51) Sivadas, N.; Daniels, M. W.; Swendsen, R. H.; Okamoto, S.; Xiao, D. Magnetic ground state of semiconducting transition-metal trichalcogenide monolayers. *Phys. Rev. B* **2015**, *91*, No. 235425.
(52) Chittari, B. L.; Park, Y.; Lee, D.; Han, M.; MacDonald, A. H.; Hwang, E.; Jung, J. Electronic and magnetic properties of single-layer m P X 3 metal phosphorous trichalcogenides. *Phys. Rev. B* **2016**, *94*, No. 184428.
(53) Jiang, P.; Wang, C.; Chen, D.; Zhong, Z.; Yuan, Z.; Lu, Z.-Y.; Ji, W. Stacking tunable interlayer magnetism in bilayer CrI 3. *Phys. Rev. B* **2019**, *99*, No. 144401.

https://doi.org/10.1021/acsomega.4c02708
ACS Omega 2024, 9, 34589−34596